Reviews in Cardiovascular Medicine

Rev. Cardiovasc. Med. **2022**; 23(3): 092
https://doi.org/10.31083/j.rcm2303092

Original Research

Comparison of Different Thoracic Aortic Wall Characteristics for Assessment of Disease Activity in Takayasu Arteritis: A Quantitative Study with 3.0 T Magnetic Resonance Imaging

Nan Zhang[1,2], Lili Pan[3], Jiayi Liu[2], Yu Li[4], Lei Xu[2], Zhonghua Sun[5,6,*], Zhenchang Wang[1,*]

[1]Department of Radiology, Beijing Friendship Hospital, Capital Medical University, 100050 Beijing, China
[2]Department of Radiology, Beijing Anzhen Hospital, Capital Medical University, 100029 Beijing, China
[3]Department of Rheumatology and Immunology, Beijing Anzhen Hospital, Capital Medical University, 100029 Beijing, China
[4]Department of Radiology, The Seventh Affiliated Hospital of Sun Yat-sen University, 518038 Shenzhen, Guangdong, China
[5]Discipline of Medical Radiation Science, Curtin Medical School, Curtin University, 6845 Perth, Australia
[6]Curtin Health Innovation Research Institute (CHIRI), Faculty of Health Sciences, Curtin University, 6845 Perth, Australia
*Correspondence: cjr.wzhch@vip.163.com (Zhenchang Wang); Z.Sun@curtin.edu.au (Zhonghua Sun)
Academic Editor: Carmela Rita Balistreri
Submitted: 15 January 2022 Revised: 11 February 2022 Accepted: 16 February 2022 Published: 9 March 2022

Abstract

Background: Determination of disease activity in Takayasu arteritis (TAK) is crucial for clinical management but challenging. The value of different magnetic resonance imaging (MRI) characteristics for the assessment of disease activity remains unclear. This study investigated the imaging findings of the thoracic aortic wall and elasticity by using a comprehensive 3.0 T MRI protocol. **Methods**: We prospectively enrolled 52 consecutive TAK patients. TAK activity was recorded according to the ITAS2010. All the patients underwent thoracic aortic MRI. The luminal morphology of the thoracic aorta and its main branches were quantitatively evaluated using a contrast-enhanced magnetic resonance angiography (MRA) sequence. The maximum wall thickness of the thoracic aorta, postcontrast enhancement ratio, and aortic wall edema were analyzed in each patient through pre- and post-enhanced T1-weighted and T2-weighted imaging. Pulse-wave velocity (PWV) of the thoracic aorta was calculated using a four-dimensional flow technique. **Results**: The majority of the 52 patients had type V disease (34.62%, 18/52). Among all the MRI indicators of the thoracic aorta, the area under the curve was the largest for the maximal wall thickness (0.804, 95% confidence interval [CI] = 0.667–0.941). The maximal wall thickness (93.33%, 95% CI = 68.1%–99.8%) exhibited the highest sensitivity with a cutoff value of 3.12 mm. Wall edema (84.00%, 95% CI = 63.9%–95.5%) presented the highest specificity. A positive correlation was noted between PWV and patients' age ($r = 0.54$, $p < 0.001$), disease duration ($r = 0.52$, $p < 0.001$), and the maximum wall thickness ($r = 0.45$, $p = 0.001$). **Conclusions**: MRI enabled the comprehensive assessment of aortic wall morphology and functional markers for TAK disease activity. Aortic maximal wall thickness was the most accurate indicator of TAK activity. The early phase was superior to the delay phase for aortic wall enhancement analysis for assessing TAK activity.

Keywords: takayasu arteritis; magnetic resonance imaging; 4D-flow; PWV; aorta

1. Introduction

Takayasu arteritis (TAK) is a form of large-vessel vasculitis of unknown etiology. Precise examination of disease activity in patients with TAK is crucial for management. Disease remission should be achieved and maintained prior to and after surgery [1].

Evaluation of disease activity in patients with TAK remains clinically challenging. The National Institute of Health activity criteria [2] and the Birmingham Vasculitis Activity Score (BVAS) [3] have been traditionally used to examine disease activity. In the past decade, a new Indian Takayasu clinical activity score (ITAS2010) was developed for assessing TAK activity on the basis of clinical symptoms and laboratory findings determined using the BVAS [4]. However, inconsistency was noted in a substantial proportion of patients with TAK in terms of their active symptoms, serum acute phase reactant levels, and radiological inflammation. Hence, the accuracy of the clinical activity score remains suboptimal.

Various imaging modalities including ultrasonography, computed tomography angiography (CTA), magnetic resonance imaging (MRI), and ^{18}F-fluorodeoxyglucose–positron emission tomography (FDG-PET) have been employed to examine disease activity. These modalities can distinguish disease activity from damage. Ultrasound, CTA, and MRI can accurately evaluate the morphology of the arterial wall and lumen. By contrast, ultrasonography is mainly used for evaluating peripheral arteries, especially the carotid artery in patients with TAK. The maximum intima-media thickness determined through ultrasonography is a favorable indicator of TAK activity [5]. Obvious contrast-enhanced ultrasound vascularization reflects TAK activity [6]. In addition, arterial wall thickness and enhancement and characteristic CTA findings (e.g., low-

attenuation ring and aortic positive remodeling) can indicate TAK activity [7]. Uptake of FDG-PET exhibited the highest sensitivity for determining TAK activity but lacked specificity [8,9]. Furthermore, arterial wall edema, which can be observed through T2-weighted imaging (T2WI) and diffused weighted imaging (DWI) with MRI, is a specific indicator of TAK activity [10,11]. The four-dimensional flow technique with MRI can be employed to evaluate hemodynamics and elasticity. Pulse-wave velocity (PWV) is associated with TAK activity [12,13]. However, the value of different MRI findings for the examination of disease activity remains unclear. Moreover, a standard MRI scan protocol for clinical use is not available. Furthermore, studies using 3.0 T MRI are limited. This study investigated the imaging findings of the thoracic aortic wall and elasticity by using a comprehensive 3.0 T MRI protocol. The clinical value of MRI findings for determining TAK activity was compared using ITAS2010 clinical activity as the reference standard.

2. Materials and Methods

2.1 Study Participants

This prospective single-center study was approved by our institutional review board. Written informed consent was obtained from each participant. Between June 2014 and December 2018, we enrolled 52 consecutive patients, including 18 first diagnosed and 34 revisited patients with TAK in this study. The definitive diagnosis of TAK was based on the 1990 American College of Rheumatology criteria [14]. TAK activity was examined according to the ITAS2010 [4]. All patients had been treated with glucocorticoids and immunosuppressive agents. High dose glucocorticoid therapy (40–60 mg/day) was used for induction of remission in the active TAK patients. Once remission occurred, the glucocorticoid dose was tailored to a target dose of 15–20 mg/day within 2–3 months and to $\leq$10 mg/day after 1 year. According to clinical data and routine imaging findings, including those of ultrasonography, CTA, and MRI, the patients with TAK were classified into Types I to V [15]. We excluded nine patients because of contraindications to MRI (n = 3), contraindications to contrast media (n = 2), and poor image quality due to arrhythmia (n = 3) and poor holding of breath (n = 1). Fig. 1 depicts the study flowchart.

2.2 MRI

All MRI examinations were performed using a 3.0 T MRI scanner (Verio, Siemens, Erlangen, Germany) equipped with a 32-channel surface-phased-array coil. The coil was placed beneath the mandible bone encompassing the whole thorax. As shown in Fig. 2, a 30-min comprehensive aortic MRI protocol was designed for the patients with TAK including dark-blood T2WI; contrast-enhanced magnetic resonance angiography (CE-MRA); pre, early, and delayed gadolinium enhanced T1-weighted imaging (T1WI); and 4D flow sequence.

Dark-blood T2WI was performed in the axis orientation with a fat sat turbo spin echo (TSE) sequence (thickness = 5 mm, slice gap = 0 mm, time to echo/time to repetition (TE/TR) = 79.0 ms/4891.9 ms, field of view (FOV) = 38 $\times$ 28.5 cm^2, and matrix = 320 $\times$ 168). Electrocardiography (ECG) and breathing trigger were adopted to minimize cardiac and respiration artifacts.

A breath-holding 3D gradient-echo (fast low-angle shot, FLASH) sequence (TE/TR = 1.1 ms/3.1 ms, FOV = 38.0 $\times$ 30.8 cm^2, matrix = 384 $\times$ 281, slice thickness = 1.2 mm, and 104 slices per slab) was used to acquire CE-MRA in coronal orientation before and after administering the contrast medium. K-space was filled by adopting the central first approach. A postcontrast scan was performed after the intravenous administration of gadopentetate dimeglumine (Magnevist, Bayer, 0.2 mmol/kg body weight, 2 mL/s) with 30 mL of saline flush at the same injection rate. The optimal acquisition time was determined using a bolus-tracking sequence.

For T1WI, a three-dimensional fat-sat-gradient recall echo volumetric interpolated breath-hold examination (VIBE; TE/TR = 1.4 ms/3.9 ms, FOV = 38.0 $\times$ 30.8 cm^2, matrix = 320 $\times$ 182, slice thickness = 3.5 mm, and 72 slices per slab) was performed in axis orientation. Early and delay enhanced images were acquired 1 and 15 min after contrast injection, respectively.

The 4D flow sequence covered the whole thoracic aorta with oblique coronal orientation in prospectively ECG-gated and navigation techniques (temporal resolution = 47.2 ms, slice thickness = 1.8 mm, TE/TR = 2.8 ms/47.2 ms, FOV = 34.0 $\times$ 25.5 cm^2, and matrix = 192 $\times$ 115). Subsequently, a two-dimensional phase-contrast cine MRI was performed to acquire optimal velocity encoding (VENC) before the 4D flow sequence. The VENC value was 100–200 cm/s, which was determined using the maximum flow velocity measured in the thoracic aortic lumen. The acquisition time for the 4D flow sequence was 6–9 min.

2.3 Image Analysis

All the acquired images were evaluated by a radiologist (N.Z.) with 11 years of experience in cardiovascular imaging. The radiologist was blinded to clinical findings.

2.4 Aortic MRA Analysis

Image postprocessing and evaluation were performed on a Siemens workstation (SyngoMMWP VE40A, Siemens Med Service Software, Erlangen, Germany). Stenosis and dilation of different arterial segments were evaluated by comparing the diameter of the diseased segment with the luminal diameter of the adjacent normal-caliber arterial segment. Pathological entities of each arterial segment were classified as stenosis, occlusion, and dilatation. Ten arterial segments were evaluated for each patient including bilateral subclavian arteries, brachiocephalic trunk (BT), bilat-

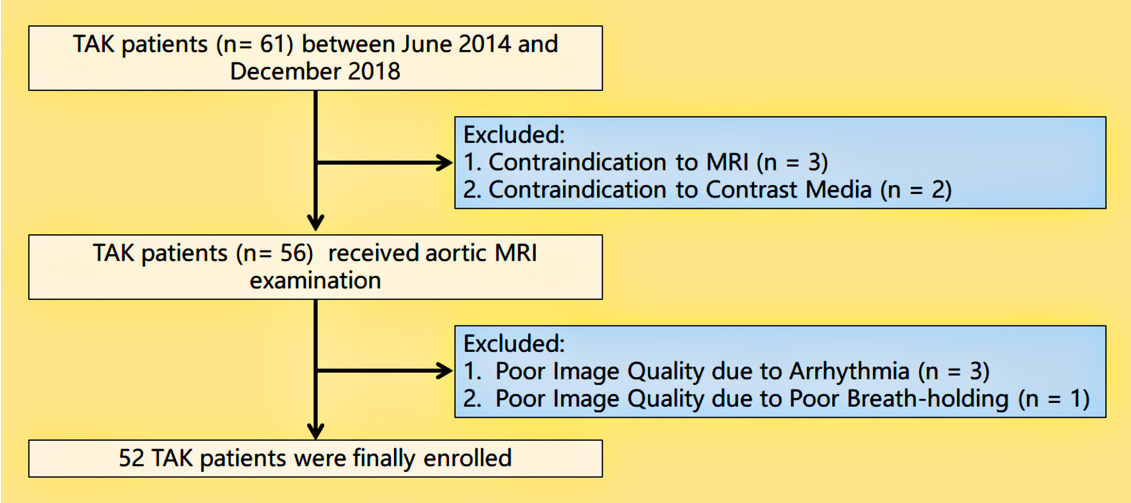

Fig. 1. Flowchart for the selection and analysis of patients with TAK (n = 52). After excluding 9 patients, a total of 52 cases with TAK were included in the analysis.

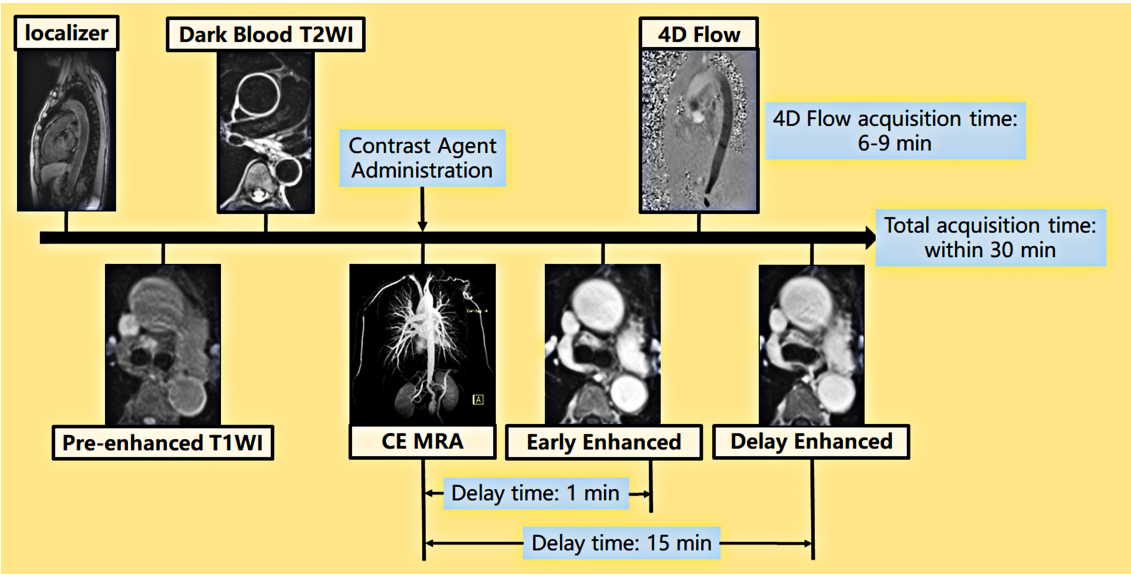

Fig. 2. Comprehensive aortic MRI protocol for patients with TAK. Pre-enhanced T1WI and dark-blood T2WI with transversal orientation performed after localization. CE-MRA was performed using the bolus-tracking sequence after contrast injection. Early and late enhanced T1WI were performed 1 and 15 min after contrast injection, respectively, with the repetition of pre-enhanced T1WI. Within the delayed period, a 4D flow sequence was performed for a duration of 6–9 min.

eral common carotid arteries (CA), bilateral vertebral arteries (VA), ascending aorta (AA), aortic arch, and descending aorta (DA).

2.5 Aortic Wall Analysis

Image postprocessing and evaluation were performed on a Siemens workstation (SyngoMMWP VE40A, Siemens Med Service Software). The following parameters were evaluated:

• Maximum wall thickness of the thoracic aorta: The aortic wall thickness was examined at the thickest site in thoracic aorta by using dark-blood T2WI.

• Postcontrast enhancement ratio: Regions of interest (ROIs) with a size of 5 to 12 pixels were set on the thickest aortic wall in pre-, early, and delay enhanced T1WI, avoiding the adjacent intra- and extra-luminal tissue and artifact. Additional ROIs were designated on the left erector spinae muscle at the same slice. The signal intensity ratio (SIR) and enhanced SIR (ESIR) of the aortic wall to the adjacent muscle were calculated as follows.

$$SIR = \frac{SI_A}{SI_M} \quad (1)$$

where SI_A is the SI of the thickest aortic wall on enhanced

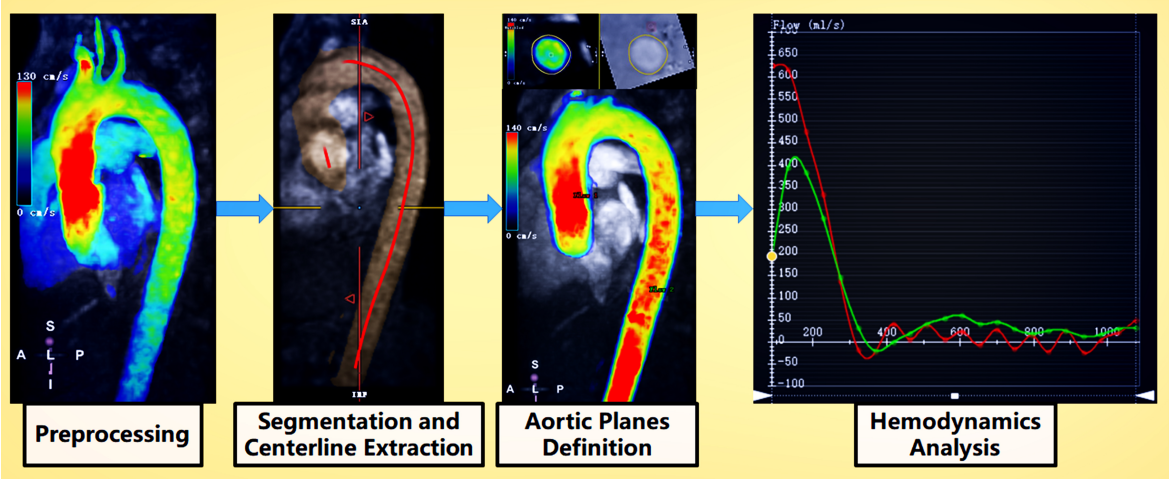

Fig. 3. 4D flow MRI analysis workflow. During preprocessing, the vessel area was masked for offset correction. Then, an antialiasing algorithm was used if the aliasing artifact existed in the flow region. Segmentation and centerline extraction were performed to define one mask with a threshold and the manual modification of the flow region. The centerline of the aorta was determined using the 2-point or multipoint method. Aortic plane selection: An appropriate plane of the aorta perpendicular to the centerline was selected and the contour of the aorta was manually modified. Hemodynamic analysis: Hemodynamic parameters (e.g., flow and velocity) were automatically acquired through the defined planes. PWV was automatically calculated using the phase shifting of profiles and the length between two planes along the centerline.

T1WI and SI_M is the SI of the left erector spinae muscle in the same slice on enhanced T1WI.

$$ESIR = \frac{SI_A - SI_{Apre}}{SI_M - SI_{Mpre}} \quad (2)$$

where SI_A is the SI of the thickest aortic wall on enhanced T1WI; SI_{Apre} is the SI on the thickest aortic wall in pre-enhanced T1WI; SI_M is the SI on the left erector spinae muscle in the same slice on enhanced T1WI; and SI_{Mpre} is the SI on the left erector spinae muscle in the same slice on pre-enhanced T1WI.

• Aortic wall edema: The presence of aortic wall edema was considered when a high SI was noted in the thickened aortic wall on dark-blood T2WI.

2.6 PWV Analysis

The 4D flow data were analyzed using a specialized module from CVI42 software (V5.13.7, Circle, Calgary, AB, Canada) [16]. After offset correction and antialiasing during preprocessing, the entire thoracic aorta was segmented and centerline extraction was semiautomatically performed through manual modification. Subsequently, for quantitative analysis, aortic 4D flow data were acquired from the aortic root to the distal descending aorta. A semi-automatic contour detection algorithm with manual verification was used to identify the aortic plane perpendicular to the aortic centerline. PWV was automatically calculated for each patient after placing two planes at the aortic root and distal descending aorta, respectively (Fig. 3).

2.7 Statistical Analysis

Statistical analysis was performed using MedCalc statistical software, version 20.019 (MedCalc Software Ltd, Ostend, Belgium). Continuous variables are expressed as the mean ± standard error or a median with 25%–75% interquartile range. Categorical variables are expressed as absolute numbers and percentages. Distribution of the normality of continuous variables was examined using the Kolmogorov–Smirnov test. Normally distributed variables were compared using the independent sample *t* test. Non-normally distributed variables were compared using the Mann–Whitney U test for the two groups. Categorical variables were compared using the chi-squared test. The correlation of PWV with age, disease duration, maximum wall thickness of the thoracic aorta, and delay ESIR was analyzed using Pearson's correlation test. Receiver-operating characteristic (ROC) curve analysis was performed to compare the diagnostic performance of the maximum wall thickness of the thoracic aorta, aortic wall edema, early ESIR, the PWV of the thoracic aorta, erythrocyte sedimentation rate (ESR), and C-reactive protein (CRP). The best cutoff values were determined using Youden's index. A p value of <0.05 was considered statistically significant.

3. Results

3.1 Study Population Characteristics

A total of 52 patients were enrolled in this study including 23 and 29 patients with active and inactive TAK, respectively, according to ITAS2010/ITAS.A. The majority of the patients were classified as type V (34.62%, 18/52),

Table 1. Clinical characteristics of the study population.

Parameter		Total (n = 52)	Active (n = 23)	Inactive (n = 29)	*p*
Demographics	Female, n (%)	49 (94.23)	21 (91.30)	28 (96.55)	0.836
	Age (y)	38.19 ±12.66	39.30 ± 14.16	37.31 ± 11.51	0.574
	Disease duration (y)	6.77 ± 6.60	7.50 ± 8.44	6.23 ± 4.96	0.747
	ESR (mm/h)	11.70 ± 9.53	17.83 ± 11.30	7.46 ± 4.87	0.000
	CRP (mg/L)	7.61 ± 18.86	17.20 ± 27.06	0.97 ± 1.15	0.000
Takayasu Clinical Activity Score	ITAS2010, median (IQR)	3.00 (0.25–8.50)	6.00 (4.00–11.50)	0.00 (0.00–1.00)	0.000
	ITAS.A, median (IQR)	4.00 (1.00–10.00)	9.00 (5.00–11.50)	0.00 (0.00–1.00)	0.000
Classification	I, n (%)	9 (17.31)	2 (8.70)	7 (24.14)	0.348
	IIa, n (%)	5 (9.62)	3 (13.04)	2 (6.90)	
	IIb, n (%)	14 (26.92)	5 (21.74)	9 (31.03)	
	III, n (%)	5 (9.62)	2 (8.70)	3 (10.34)	
	IV, n (%)	1 (1.92)	0 (0.00)	1 (3.45)	
	V, n (%)	18 (34.62)	11 (47.83)	7 (24.14)	

IQR, interquartile range; ESR, erythrocyte sedimentation rate; CRP, C-reactive protein.

followed by type IIb (26.92%, 14/52). In this cohort, 94.23% (49/52) of the patients were women with a mean age of 38.19 ± 12.66 years. No significant differences in sex, age, disease duration, and classification were observed between the active and inactive groups. Compared with the inactive group, the active group had higher ESR (17.83 ± 11.30 mm/h vs. 7.46 ± 4.87 mm/h, $p < 0.001$), CRP levels (17.20 ± 27.06 mg/L vs. 0.97 ± 1.15 mg/L, $p < 0.001$), and Takayasu clinical activity scores (ITAS2010: 6.00 vs. 0.00, $p < 0.001$; ITAS.A: 9.00 vs. 0.00, $p < 0.001$). Table 1 lists the clinical characteristics of the study population.

3.2 Thoracic Aortic MRA

A total of 520 arterial segments were evaluated in the 52 patients. Arterial pathologies were noted in 193 segments (96 and 97 segments in the active and inactive groups, respectively), including 123 stenosed, 51 occlusive, and 19 dilated segments. The left subclavian artery (44/52, 84.62%) was the most commonly involved segment, followed by the right subclavian artery (38/52, 73.08%) and the left common carotid artery (33/52, 63.46%). Arterial dilation was more common in the aorta (12 segments) including 7 segments of the ascending aorta, 2 segments of the aortic arch, and 3 segments of the descending aorta. Table 2 presents the details of these pathologies.

3.3 Aortic Wall Imaging

The maximum wall thickness of the thoracic aorta was significantly larger in the active group (3.89 ± 1.50 mm vs. 3.00 ± 1.04 mm, $p = 0.009$; Table 3). Compared with the inactive group, more patients in the active group exhibited a high SI at the aortic wall (56.5% [13/23] vs. 17.2% [5/29], $p = 0.003$) on T2WI images, indicating the presence of aortic wall edema. In the early enhanced scan, the postcontrast enhancement ratio was significantly higher in the active group when weighted with ESIR (2.63 ± 2.14 vs. 1.11 ± 1.04, $p = 0.013$). Although aortic SIR and ESIR were higher in the active TAK group in delay enhanced images, no significant difference was observed between the active and inactive TAK groups. Fig. 4 presents the findings of a patient with active TAK.

3.4 PWV of the Thoracic Aorta

The PWV of the thoracic aorta in this cohort was 8.55 ± 4.57 m/s and significantly differed between the active and inactive TAK groups. Compared with the inactive TAK group, the active TAK group had a significantly higher PWV (10.45 ± 5.11 m/s vs. 7.20 ± 3.66 m/s, $p = 0.016$). A positive correlation was noted between PWV and patients' age (r = 0.54, 95% CI = 0.27–0.73, $p < 0.001$), disease duration (r = 0.52, 95% CI = 0.25–0.71, $p < 0.001$), maximum wall thickness of the thoracic aorta (r = 0.45, 95% CI = 0.19–0.65, $p = 0.001$). However, a negative correlation was noted between the PWV and delay enhanced ESIR (r = –0.33, 95% CI = –0.59 to –0.0068, $p = 0.046$; Fig. 5).

3.5 ROC Analysis

Among all the MRI indicators of the thoracic aorta, the area under the curve (AUC) was the largest for the maximal wall thickness (0.804, 95% CI = 0.667–0.941). According to the ROC curve analysis of these MRI indicators, the cutoff values of the maximal wall thickness, early enhanced ESIR, and PWV were 3.12 mm, 1.13, and 6.4 m/s, respectively. On the basis of these cutoff values, the maximal wall thickness exhibited the highest sensitivity for the determination of active TAK (93.33%, 95% CI = 68.1%–99.8%), whereas wall edema demonstrated the highest specificity (84.00%, 95% CI = 63.9%–95.5%; Table 4).

ESR (0.851, 95% CI = 0.733–0.969) and CRP levels (0.808, 95% CI = 0.647–0.969) were superior to the MRI indicators of the thoracic aorta for determining the clinical activity of TAK (Fig. 6).

Table 2. Arterial pathologies in aortic branches between the active and inactive TAK groups.

Arteries	Degree of stenosis	Total (n = 52)	Active (n = 23)	Inactive (n = 29)
RSCA	stenosis	23 (44.23)	13 (56.52)	10 (34.48)
	occlusion	10 (19.23)	3 (13.04)	7 (24.14)
	dilatation	5 (9.62)	1 (4.35)	4 (13.79)
LSCA	stenosis	23 (44.23)	14 (60.87)	9 (31.03)
	occlusion	20 (38.46)	10 (43.48)	10 (34.48)
	dilatation	1 (1.92)	1 (4.35)	0
BT	stenosis	10 (19.23)	4 (17.39)	6 (20.69)
	occlusion	1 (1.92)	1 (4.35)	0
	dilatation	1 (1.92)	0	1 (3.45)
RCA	stenosis	15 (28.85)	6 (26.09)	9 (31.03)
	occlusion	7 (13.46)	4 (17.39)	3 (10.34)
	dilatation	0	0	0
LCA	stenosis	25 (48.08)	12 (52.17)	13 (44.83)
	occlusion	8 (15.38)	4 (17.39)	4 (13.79)
	dilatation	0	0	0
RVA	stenosis	6 (11.54)	4 (17.39)	2 (6.90)
	occlusion	2 (3.85)	1 (4.35)	1 (3.45)
	dilatation	0	0	0
LVA	stenosis	4 (7.69)	3 (13.04)	1 (3.45)
	occlusion	3 (5.77)	1 (4.35)	2 (6.90)
	dilatation	0	0	0
AA	stenosis	1 (1.92)	1 (4.35)	0
	occlusion	0	0	0
	dilatation	7 (13.46)	5 (21.74)	2 (6.90)
Aortic arch	stenosis	2 (3.85)	1 (4.35)	1 (3.45)
	occlusion	0	0	0
	dilatation	2 (3.85)	1 (4.35)	1 (3.45)
DA	stenosis	14 (26.92)	4 (17.39)	10 (34.48)
	occlusion	0	0	0
	dilatation	3 (5.77)	2 (8.70)	1 (3.45)

RSCA, right subclavian artery; LSCA, left subclavian artery; BT, brachiocephalic trunk; RCA, right common carotid artery; LCA, left common carotid artery; RVA, right vertebral artery; LVA, left vertebral artery; AA, ascending aorta; DA, descending aorta.

4. Discussion

In this study, we used a comprehensive MRI protocol of the thoracic aorta to determine the morphological and functional characteristics of the aortic wall. We examined whether these characteristics can be used to assess disease activity in 52 patients with TAK. The maximal wall thickness was the most favorable indicator for determining TAK activity with the highest sensitivity. Aortic wall edema can be used as a specific marker to detect TAK activity with high specificity. Compared with delay enhancement, early-enhanced ESIR was a better indicator of TAK activity. Furthermore, by using the 4D flow technique, aortic PWV could be determined to detect active TAK with high sensitivity.

Accurate assessment of TAK activity is crucial for clinical management but remains challenging with the current approaches. Studies have investigated TAK activity by using different imaging modalities. Ultrasound is a convenient and cheap imaging method that is the most widely used in clinical practice to evaluate the peripheral arteries of patients with TAK. Characteristic thickening of the carotid arterial wall is an accurate diagnostic clue for TAK disease. The maximum intima-media thickness and contrast-enhanced ultrasound can be reliable indicators for detecting disease activity. However, the difficulty of aortic wall assessment limits the usage of ultrasound in patients with TAK with aorta involvement. CTA allows the visualization of the lumen and wall of variable arteries in the whole body.

Table 3. Aortic wall imaging findings between the active and inactive groups.

Parameters		Total (n = 52)	Active (n = 23)	Inactive (n = 29)	*p*
Thickness (mm)		3.39 ± 1.33	3.89 ± 1.50	3.00 ± 1.04	0.009
Edema, n (%)		18 (34.6)	13 (56.5)	5 (17.2)	0.003
Early enhanced	SIR	1.36 ± 0.53	1.50 ± 0.59	1.20 ± 0.43	0.126
	ESIR	1.75 ± 1.76	2.63 ± 2.14	1.11 ± 1.04	0.013
Delay enhanced	SIR	1.86 ± 0.47	1.95 ± 0.48	1.76 ± 0.46	0.189
	ESIR	3.71 ± 1.54	4.04 ± 1.74	3.35 ± 1.24	0.313
PWV (m/s)		8.55 ± 4.57	10.45 ± 5.11	7.20 ± 3.66	0.016

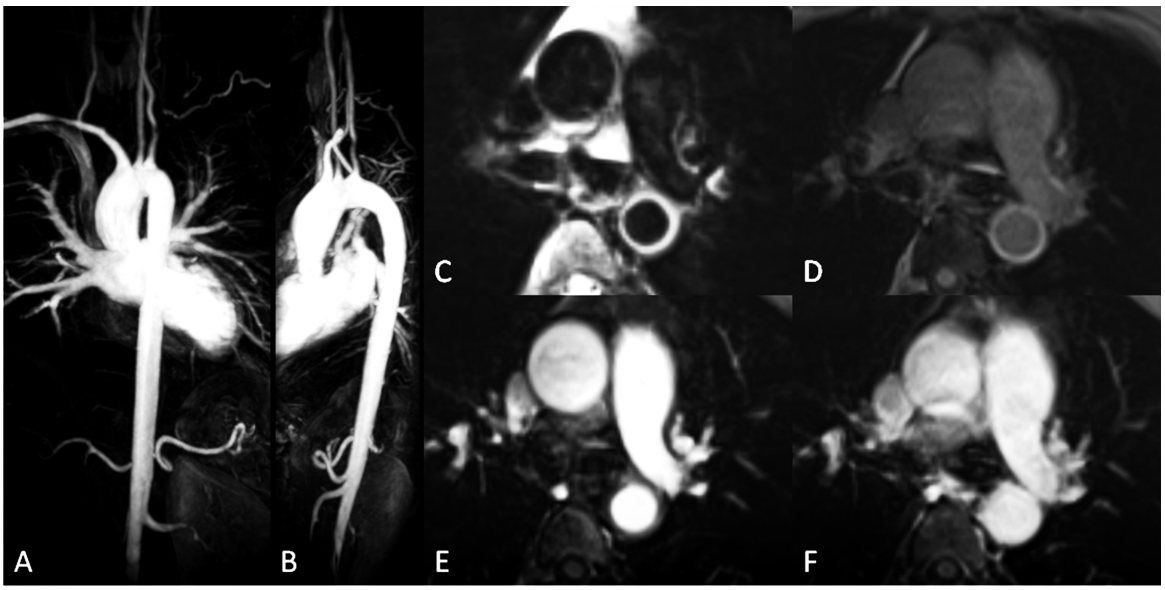

Fig. 4. MRI findings of a 32-year-old female patient with active TAK with an ITAS2010 score of 10, an ESR of 14 mm/h, and a CRP level of 32.16 mg/L. (A,B) CE-MRA showed occlusive lesions at the LSCA, RCA, and right renal artery. Significant stenosis was observed at the RSCA. (C) T2WI showed a thickened descending aortic wall with obvious edema. The thickness of the descending aortic wall was 4.65 mm. (D–F) Early and delay enhancement of the thickened descending aortic wall were observed with an early SIR of 2.20, an early ESIR of 5.46, a delay SIR of 2.95, and a delay ESIR of 6.84.

The high spatial resolution of CTA enables the quantitative assessment of morphological characteristics. Arterial wall thickness, wall enhancement, low-attenuation ring, and aortic positive remodeling are the indicators of TAK activity. Use of ionizing radiation and iodinated contrast agents raise concerns in patients with TAK with renal dysfunction or those requiring regular follow-up imaging. FDG-PET is the most sensitive imaging modality for detecting active local inflammatory changes in the aortic and peripheral arterial wall [8,9]. However, the use of FDG-PET is hindered by its high cost, ionizing radiation, low specificity, and low spatial resolution.

Because of its ability to accurately examine soft tissue characteristics and the availability of a range of dedicated sequences, MRI has been widely used in clinical practice for the assessment of TAK activity [8]. Similar to CTA, MRI enables accurate whole-body vascular characterization [17]. Stenosis, occlusion, and dilation of systemic arteries can be quantitatively evaluated through MRA. Information on the involved arterial site, extent, and degree can be obtained with high reproducibility. With the development of the MRI technique, 2D or 3D multi-weighted vessel wall imaging can be used for examining the whole-body vascular structure. Thus, MRI is useful for early diagnosis, activity assessment, and relapse identification in patients with TAK. Functional evaluation of the aorta, including its hemodynamic and elasticity, can provide additional information regarding activity and prognosis. Hence, a comprehensive MRI protocol was used in this study for examining patients with TAK.

TAK is a form of large-vessel arteritis including the aorta, aortic primary branches, coronary arteries, and pulmonary arteries. Active arterial lesions can be solitary, diffuse, or multiple. Thus, for accurate TAK activity assessment, arteries in the whole body should be evaluated. Difficulty in examining all diseased arterial segments can lead

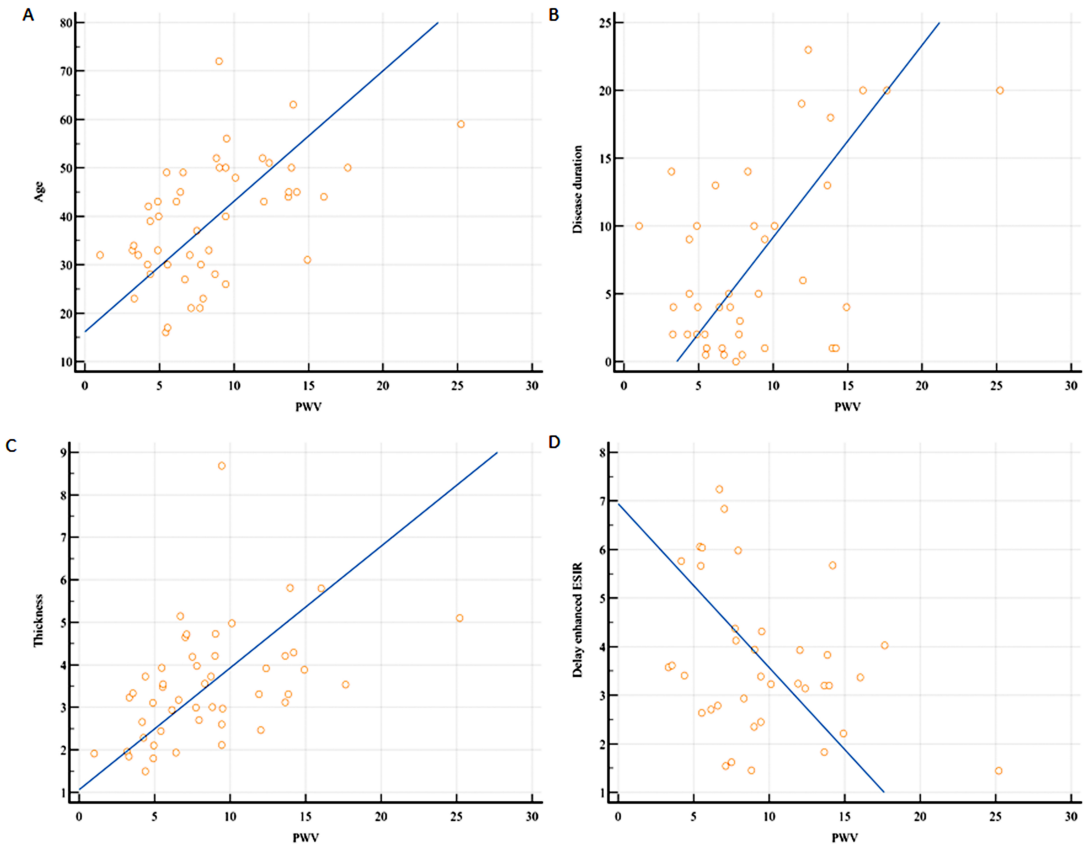

Fig. 5. Correlation between PWV and different parameters. (A–C) A positive correlation existed between PWV and patient's age (r = 0.54, 95% CI = 0.27–0.73, $p < 0.001$), disease duration (r = 0.52, 95% CI = 0.25–0.71, $p < 0.001$), maximum wall thickness of the thoracic aorta (r = 0.45, 95% CI = 0.19–0.65, $p = 0.001$). (D) A negative correlation existed between the PWV and delay enhanced ESIR (r = –0.33, 95% CI = –0.59 to –0.0068, $p = 0.046$).

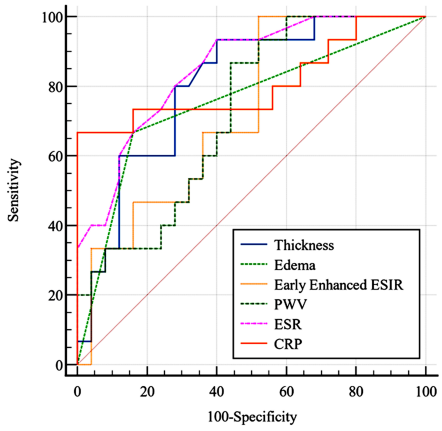

Fig. 6. AUC determined through the ROC analysis of MRI indicators. ESR (0.851, 95% CI = 0.733–0.969) and CRP (0.808, 95% CI = 0.647–0.969) were superior to each thoracic aortic wall characteristic for the assessment of TAK activity. Among all MRI findings, AUC was the largest for the maximal wall thickness (0.804, 95% CI = 0.667–0.941).

to a decreased sensitivity of TAK activity assessment. Because of the time-consuming nature and magnetic field inhomogeneity of the 3.0 T system, only the thoracic aortic wall was evaluated for determining the clinical activity of the patients with TAK in this study. Although the majority of the patients in the cohort had type V disease (34.62%, 18/52) with the simultaneous involvement of the carotid arteries, thoracic aorta, and abdominal aorta, the largest AUC of MRI indicators reached 0.804 (95% CI = 0.667–0.941) in the maximal thoracic aortic wall thickness. When considering the whole aorta, in a CTA study [7], the AUC of the maximal aortic wall thickness for determining TAK activity reached 0.906 (95% CI = 0.850–0.946). In addition to the aorta, carotid intima-media thickness measured through ultrasound and ^{18}F-FDG uptake of the pulmonary artery in FDG-PET exhibited a satisfactory correlation with disease activity [18,19].

Arterial wall thickening, edema, and contrast enhancement were correlated with active vascular inflammation in patients with TAK, as determined through MRI [10,17,20–26]. When FDG-PET was used to determine activity, aortic wall edema with a high SI on T2WI was independently associated with FDG uptake [27]. In this

Table 4. Diagnostic value of MRI indicators.

Parameter	AUC (95% CI)	Sensitivity (95% CI)	Specificity (95% CI)	Cut off value	*p*
Thickness (mm)	0.804 (0.667–0.941)	93.33 (68.1–99.8)	60.00 (38.7–78.9)	3.12	0.001
Edema	0.753 (0.587–0.919)	66.67 (38.4–88.2)	84.00 (63.9–95.5)	-	0.001
Early enhanced ESIR	0.723 (0.565–0.880)	66.67 (38.4–88.2)	64.00 (42.5–82.0)	1.13	0.006
PWV (m/s)	0.723 (0.566–0.879)	86.67 (59.5–98.3)	56.00 (34.9–75.6)	6.4	0.006
ESR (mm/h)	0.851 (0.733–0.969)	77.78 (52.4–93.6)	84.62 (65.1–95.6)	20	0.001
CRP (mg/L)	0.808 (0.647–0.969)	69.23 (48.2–85.7)	83.33 (58.6–96.4)	5	0.001

study, the diagnostic accuracy of thoracic aortic wall edema for TAK activity was evaluated by performing ROC analysis. The AUC reached 0.753 (95% CI = 0.587–0.919) with a sensitivity of 66.67% (95% CI = 38.4%–88.2%) and a specificity of 84.00% (95% CI = 63.9%–95.5%). Yang *et al.* [10] demonstrated that low b-value DWI was superior to T2WI in identifying aortic wall inflammation in patients with active TAK. The findings of TAK activity assessment performed using arterial wall contrast enhancement have been inconsistent. Most of the researchers have indicated that aortic wall contrast enhancement on MRI findings is suggestive of active TAK [10,21,22,28,29]. Kato *et al.* [26] reported that 30-min late gadolinium enhancement (LGE) with the Look–Locker inversion-recovery sequence was useful for the detection of arterial wall involvement. However, TAK activity could not be determined through LGE. The inconsistency in the results may be due to the use of varying delay scan times, imaging techniques, and definitions of active TAK. Choe *et al.* [28] observed the early (delay within 5 min), intermediate (delay of 5–10 min), and late (delay of 10–20 min) contrast enhancement patterns of the aortic wall in patients with TAK by using spin-echo T1WI images. Increased enhancement was noted in patients with active TAK on early, intermediate, and late enhanced scans. However, only the early contrast enhancement of the aortic wall was well-correlated with the ESR ($r = 0.78$, $p < 0.005$) and CRP ($r = 0.63$, $p < 0.005$). In this study, we performed a post contrast-enhanced scan at 1 and 15 min by using the VIBE technique. Compared with the inactive TAK group, the active TAK group exhibited a significantly increased ESIR on early enhanced images (2.63 ± 2.14 vs. 1.11 ± 1.04, $p = 0.013$). With a cutoff value of 1.13, early enhanced ESIR could identify active TAK with an AUC of 0.723 (95% CI = 0.565–0.880), a sensitivity of 66.67% (95% CI = 38.4%–88.2%), and a specificity of 64.00% (42.5%–82.0%). In the early stage of TAK, the main histological findings were the perivascular cuffing of the vasa vasorum and granulomatous panarteritis [1,30]. Thus, early aortic wall enhancement might reflect active inflammation, whereas late contrast enhancement might be attributed to increased extracellular volume and diffused fibrosis in the scar stage [1,30].

Aortic PWV evaluated using the 4D flow technique was a potential indicator of TAK activity and prognosis. Brachial-ankle and carotid-femoral PWV were correlated with TAK disease activity [12,13]. Similar to arteriosclerosis, brachial-ankle PWV levels in patients with TAK were associated with major adverse cardiac events [31]. Because stenotic and occlusive lesions usually occur in the peripheral arteries in patients with TAK, aortic PWV derived from MRI can reflect arterial elastic function more accurately compared with brachial-ankle or carotid-femoral PWV. In this study, thoracic aortic PWV was significantly increased in the active TAK group (10.45 ± 5.11 m/s vs. 7.20 ± 3.66 m/s, $p = 0.016$). With a cutoff value of 6.4 m/s, PWV could identify active TAK with an AUC of 0.723 (95% CI = 0.566–0.879), a sensitivity of 86.67% (95% CI = 59.5%–98.3%), and a specificity of 56.00% (95% CI = 34.9%–75.6%). Except for age and the disease duration, a positive correlation was observed between PWV and the maximum wall thickness of the thoracic aorta. By contrast, a negative correlation was noted between PWV and delay enhanced ESIR. Wall thickening and fibrosis might be pathological factors affecting arterial elastic function in patients with TAK.

5. Limitations

This study has several limitations. First, this was a single-center study. The sample size was relatively small. Second, no follow-up MRI images were available for this cohort. Future studies with large sample sizes and follow-up data are warranted. Third, only the thoracic aorta was evaluated in this study. Whole-body MRI including the whole aorta, carotid artery, and pulmonary artery might determine TAK disease activity more accurately.

6. Conclusions

MRI enables the comprehensive evaluation of the morphological and functional features of the aortic wall that can be used for determining TAK disease activity. Among all the MRI parameters, aortic maximal wall thickness was the most accurate indicator of TAK activity. The early phase was superior to the delay phase for aortic wall enhancement analysis to determine TAK activity. Except for age and the disease duration, aortic wall thickening and fibrosis can be pathological factors for affecting arterial elastic function in patients with TAK.

Author Contributions

NZ, LP and JL—propose the concept. JL, LX and ZW—designed the research study. NZ and YL— acquired, analyzed and interpreted the data. NZ and LP—prepared the original draft. ZS and ZW—provided review and editing of the manuscript. All authors have read and agreed to the published version of the manuscript.

Ethics Approval and Consent to Participate

The study was conducted in accordance with the Declaration of Helsinki, and approved by the Institutional Review Board (or Ethics Committee) of BEIJING ANZHEN HOSPITAL, CAPITAL MEDICAL UNIVERSITY (2022023X). All subjects gave their informed consent for inclusion before they participated in the study.

Acknowledgment

Not applicable.

Funding

This study was supported by grants from Beijing Scholar 2015 (ZW), the National Natural Science Foundation of China (U1908211), the Capital's Funds for Health Improvement, and Research Foundation of China (2020-1-1052).

Conflict of Interest

The authors declare no conflict of interest. Zhonghua Sun is serving as one of the Editorial Board members/Guest editors of this journal. We declare that Zhonghua Sun had no involvement in the peer review of this article and has no access to information regarding its peer review. Full responsibility for the editorial process for this article was delegated to Carmela Rita Balistreri.

References

[1] Tombetti E, Mason JC. Takayasu arteritis: advanced understanding is leading to new horizons. Rheumatology. 2019; 58: 206–219.

[2] Kerr GS, Hallahan CW, Giordano J, Leavitt RY, Fauci AS, Rottem M, *et al*. Takayasu arteritis. Annals of Internal Medicine. 1994; 120: 919–929.

[3] Luqmani RA, Bacon PA, Moots RJ, Janssen BA, Pall A, Emery P, *et al*. Birmingham Vasculitis Activity Score (BVAS) in systemic necrotizing vasculitis. QJM: Monthly Journal of the Association of Physicians. 1994; 87: 671–678.

[4] Misra R, Danda D, Rajappa SM, Ghosh A, Gupta R, Mahendranath KM, *et al*. Development and initial validation of the Indian Takayasu Clinical Activity Score (ITAS2010). Rheumatology. 2013; 52: 1795–1801.

[5] Svensson C, Eriksson P, Zachrisson H. Vascular ultrasound for monitoring of inflammatory activity in Takayasu arteritis. Clinical Physiology and Functional Imaging. 2020; 40: 37–45.

[6] Wang Y, Wang Y, Tian X, Wang H, Li J, Ge Z, *et al*. Contrast-enhanced ultrasound for evaluating arteritis activity in Takayasu arteritis patients. Clinical Rheumatology. 2020; 39: 1229–1235.

[7] Chen B, Wang X, Yin W, Gao Y, Hou Z, An Y, *et al*. Assessment of disease activity in Takayasu arteritis: a quantitative study with computed tomography angiography. International Journal of Cardiology. 2019; 289: 144–149.

[8] Dejaco C, Ramiro S, Duftner C, Besson FL, Bley TA, Blockmans D, *et al*. EULAR recommendations for the use of imaging in large vessel vasculitis in clinical practice. Annals of the Rheumatic Diseases. 2018; 77: 636–643.

[9] Slart RHJA. FDG-PETCT(a) imaging in large vessel vasculitis and polymyalgia rheumatica: joint procedural recommendation of the EANM, SNMMI, and the PET Interest Group (PIG), and endorsed by the ASNC. European Journal of Nuclear Medicine and Molecular Imaging. 2018; 45: 1250–1269.

[10] Yang H, Lv P, Zhang R, Fu C, Lin J. Detection of mural inflammation with low b-value diffusion-weighted imaging in patients with active Takayasu Arteritis. European Radiology. 2021; 31: 6666–6675.

[11] Sarma K, Handique A, Phukan P, Daniala C, Chutia H, Barman B. Magnetic Resonance Angiography and Multidetector CT Angiography in the Diagnosis of Takayasu's Arteritis: Assessment of Disease Extent and Correlation with Disease Activity. Current Medical Imaging Reviews. 2022; 18: 51–60.

[12] Wang Z, Dang A, Lv N. Brachial-Ankle Pulse Wave Velocity is Increased and Associated with Disease Activity in Patients with Takayasu Arteritis. Journal of Atherosclerosis and Thrombosis. 2020; 27: 172–182.

[13] Salles Rosa Neto N, Levy-Neto M, Tolezani EC, Bonfá E, Bortolotto LA, Pereira RMR. Determinants of arterial stiffness in female patients with Takayasu arteritis. The Journal of Rheumatology. 2014; 41: 1374–1378.

[14] Arend WP, Michel BA, Bloch DA, Hunder GG, Calabrese LH, Edworthy SM, *et al*. The American College of Rheumatology 1990 criteria for the classification of Takayasu arteritis. Arthritis and Rheumatism. 1990; 33: 1129–1134.

[15] Hata A, Noda M, Moriwaki R, Numano F. Angiographic findings of Takayasu arteritis: New classification. International Journal of Cardiology. 1996; 54: S155–S163.

[16] Fatehi Hassanabad A, Burns F, Bristow MS, Lydell C, Howarth AG, Heydari B, *et al*. Pressure drop mapping using 4D flow MRI in patients with bicuspid aortic valve disease: a novel marker of valvular obstruction. Magnetic Resonance Imaging. 2020; 65: 175–182.

[17] Li D, Lin J, Yan F. Detecting disease extent and activity of Takayasu arteritis using whole-body magnetic resonance angiography and vessel wall imaging as a 1-stop solution. Journal of Computer Assisted Tomography. 2011; 35: 468–474.

[18] Park SH, Chung JW, Lee JW, Han MH, Park JH. Carotid artery involvement in Takayasu's arteritis: evaluation of the activity by ultrasonography. Journal of Ultrasound in Medicine. 2001; 20: 371–378.

[19] Gao W, Gong J, Guo X, Wu J, Xi X, Ma Z, *et al*. Value of 18F-fluorodeoxyglucose positron emission tomography/computed tomography in the evaluation of pulmonary artery activity in patients with Takayasu's arteritis. European Heart Journal. 2021; 22: 541–550.

[20] Direskeneli H, Aydin SZ, Merkel PA. Assessment of disease activity and progression in Takayasu's arteritis. Clinical and Experimental Rheumatology. 2011; 29: S86–S91.

[21] John RA, Keshava SN, Danda D. Correlating MRI with clinical evaluation in the assessment of disease activity of Takayasu's arteritis. International Journal of Rheumatic Diseases. 2017; 20: 882–886.

[22] Jiang L, Li D, Yan F, Dai X, Li Y, Ma L. Evaluation of Takayasu arteritis activity by delayed contrast-enhanced magnetic resonance imaging. International Journal of Cardiology. 2012; 155: 262–267.

[23] Kenar G, Karaman S, Cetin P, Yarkan H, Akar S, Can G, et al. Imaging is the major determinant in the assessment of dis-

ease activity in Takayasu's arteritis. Clinical and Experimental Rheumatology. 2020; 38: 55–60.

[24] Barra L, Kanji T, Malette J, Pagnoux C. Imaging modalities for the diagnosis and disease activity assessment of Takayasu's arteritis: a systematic review and meta-analysis. Autoimmunity Reviews. 2018; 17: 175–187.

[25] Sun Y, Huang Q, Jiang L. Radiology and biomarkers in assessing disease activity in Takayasu arteritis. International Journal of Rheumatic Diseases. 2019; 22: 53–59.

[26] Kato Y, Terashima M, Ohigashi H, Tezuka D, Ashikaga T, Hirao K, *et al*. Vessel Wall Inflammation of Takayasu Arteritis Detected by Contrast-Enhanced Magnetic Resonance Imaging: Association with Disease Distribution and Activity. PloS ONE. 2015; 10: e0145855.

[27] Quinn KA, Ahlman MA, Malayeri AA, Marko J, Civelek AC, Rosenblum JS, *et al*. Comparison of magnetic resonance angiography and 18F-fluorodeoxyglucose positron emission tomography in large-vessel vasculitis. Annals of the Rheumatic Diseases. 2018; 77: 1165–1171.

[28] Choe YH, Han BK, Koh EM, Kim DK, Do YS, Lee WR. Takayasu's arteritis: assessment of disease activity with contrast-enhanced MR imaging. American Journal of Roentgenology. 2000; 175: 505–511.

[29] Papa M, De Cobelli F, Baldissera E, Dagna L, Schiani E, Sabbadini M, *et al*. Takayasu arteritis: intravascular contrast medium for MR angiography in the evaluation of disease activity. American Journal of Roentgenology. 2012; 198: W279–W284.

[30] Ozaki S, Ando M, Isobe M, Kobayashi S, Matsunaga N, Miyata T, *et al*. Guideline for management of vasculitis syndrome (JCS 2008). Japanese Circulation Society. Circulation Journal. 2011; 75: 474–503.

[31] Wang X, Dang A. Prognostic Value of Brachial-Ankle Pulse Wave Velocity in Patients with Takayasu Arteritis with Drug-Eluting Stent Implantation. Arthritis Care & Research. 2015; 67: 1150–1157.